

# SOIL BASED DESIGN OF HIGHWAY GUARDRAIL POST DEPTHS USING PENDULUM IMPACT TESTS

# ZASNOVA GLOBINE STEBRA AVTOCESTNE OGRAJE GLEDE NA LASTNOSTI TAL Z UPORABO UDARNIH PREIZKUSOV Z NIHALOM

## Murat Örnek (corresponding author)

Iskenderun Technical University,  
Faculty of Engineering and Natural Sciences,  
Civil Engineering Department  
31200, Iskenderun, Hatay, Turkey  
E-mail: murat.ornek@iste.edu.tr

## Ali Osman Atahan

Istanbul Technical University,  
Civil Engineering Faculty,  
Civil Engineering Department  
34469, Istanbul, Turkey  
E-mail: atahana@itu.edu.tr

## Yakup Türedi

Iskenderun Technical University,  
Faculty of Engineering and Natural Sciences,  
Civil Engineering Department  
31200, Iskenderun, Hatay, Turkey  
E-mail: yakup.turedi@iste.edu.tr

## M. Musab Erdem

Iskenderun Technical University,  
Faculty of Engineering and Natural Sciences,  
Civil Engineering Department  
31200, Iskenderun, Hatay, Turkey  
E-mail: musab.erdem@iste.edu.tr

## Murat Büyük

Sabancı University,  
Integrated Manufacturing Technologies R&A Center  
34956, Istanbul, Turkey  
E-mail: muratbuyuk@sabanciuniv.edu

DOI <https://doi.org/10.18690/actageotechslov.16.2.77-89.2019>

## Keywords

guardrail; post; post embedment depth; soil properties; post-soil interaction; pendulum test

## Ključne besede

ograja; steber; globina vpetja; lastnosti tal; interakcija steber-tla; preizkus z nihalom

## Abstract

Guardrails are passive road restraint systems (RRS) used at roadsides and medians to improve road safety. In the case of inadequate post embedment depth of soil driven posts may not function as intended and design cannot provide adequate safety nor security for the impacting vehicles. In general, the height of the steel guardrails varies between 1600 and 2400mm. However, the characteristics of the soil where the guardrails are driven are not taken into consideration. In other words, a constant depth of guardrail is used regardless of the type of soil. Post embedment depths (PED) in steel guardrail systems are currently determined based on strong soil properties. The crash performance of these designs may not be appropriate for locations where soil conditions are weaker than tested conditions.

In this study, a series of field impact tests were performed on soil embedded posts to determine optimum PED for

## Izvleček

Varovalne ograje so pasivni cestni zadrževalni sistemi (RRS), ki se uporabljajo ob robovih in na sredini cest za izboljšanje varnosti v cestnem prometu. V primeru nezadostne globine vpetja stebrov, vtisnjenih v zemljinu, se lahko zgodi, da ne delujejo kot je predvideno, zato konstrukcija ne more zagotoviti zadostne varnosti ali varnosti za vozila, ki udarijo v njo. Na splošno je višina jeklene varnostne ograje med 1600 in 2400 mm. Vendar pa se lastnosti tal, v katerih so vgrajene varnostne ograje, praviloma ne upoštevajo. Z drugimi besedami, ne glede na vrsto tal, se izvaja konstantna globina vpetja stebrov zaščitne ograje. Globine vpetja stebrov (PED) v sistemih jeklenih zaščitnih ograj so trenutno določene na podlagi visokih trdnosti tal. Zmogljivost teh modelov za trk ni primerna za lokacije, kjer so trdnostne karakteristike tal nižje od predpostavljenih v osnovnem izračunu.

V tej študiji so bili opravljeni terenski udarni preizkusi na stebre vpete v tla, da bi določili optimalno globino vpetja

three different soil conditions, namely hard, medium hard and soft soil. A pendulum device is used to perform dynamic impact tests on C type (C120x60x4), H type (H150x90x6) and S type (S100x50x4.2) posts. Seven different PED values were used for each type of soil. A total of 63 impact tests proved that increased soil stiffness resulted reduction in PED for the posts. Optimum PED values are determined based on energy absorption of posts. With the use of optimum length guardrail posts considerable amount of installation time, labor and material savings are expected.

## 1 INTRODUCTION

The roadside can be defined as the area between the outside shoulder edge of a road and the right-of-way limits [1]. The utilization of engineering treatments in this area to improve traffic safety is referred to as roadside safety design and guardrails are one of the most widely used passive safety devices for roadsides.

Most guardrail designs in the world are made out of steel or concrete. Concrete barrier designs usually do not contain a foundation and they are simply placed on the road surface. Thus soil-barrier interaction is not an issue for concrete barriers. However, this is not the case for steel designs. Posts of the steel guardrail designs have to be either bolted to a concrete deck or driven into the soil. Therefore, the connection and any details of this connection have to be designed properly for a steel guardrail to perform as intended.

Steel-guardrail designs are mostly installed in soil, since the number of bridges in a standard highway project is limited. For steel guardrails' post-soil interaction the properties of the soil and the extent of the post embedment depth (PED) become essential parameters affecting the impact performance [2,5,6]. With a lack of post-soil interaction or an inadequate PED a steel guardrail might not function as intended and the design cannot provide adequate safety nor security for the impacting vehicles. In general, the height of the steel guardrails varies between 1600 and 2400 mm. However, the characteristics of the soil where the guardrails are driven are not taken into consideration. In other words, a constant depth of guardrail is used, regardless of the type of soil. Unfortunately, the PEDs in steel guardrail systems are currently determined based on strong soil properties [3]. The crash performance of these designs might not be appropriate for locations where the soil conditions are weaker than the tested conditions.

stebrov za tri različne trdnostne razmere v tleh, in sicer trdo, srednje trdo in mehko zemljinjo. Nihalno napravo uporabljamo za izvedbo dinamičnih udarnih preizkusov na stebrih tipa C (C120x60x4), H (H150x90x6) in S (S100x50x4.2). Za vsako vrsto tal je bilo uporabljenih sedem različnih vrednosti globin vpetja stebrov. Skupno je bilo tako izvedenih 63 udarnih preizkusov, s čimer se je dokazalo, da je povečana togost tal povzročila zmanjšanje globine vpetja stebrov. Optimalne vrednosti globine vpetja stebrov se določijo na podlagi absorpcije energije stebrov. Z uporabo optimalne dolžine stebrov zaščitne ograje se pričakuje precej prihranka pri času za vgradnjo, delu in materialu.

The European crash-test standard EN131 is a performance-based standard. In other words, regardless of the properties of the guardrail elements, only the impact-response behavior of the guardrail is considered [4]. The adequacy of guardrail systems is evaluated using the EN1317 standard and successful designs receive certification for highway use. This standard has been mandatory in Turkey since 2011 and it provides crash-test procedures and acceptance criteria for crash tests. Even though the guardrail post-soil interaction and the soil properties are of importance in crash tests, EN1317 does not provide detailed information on this topic. There are not many studies in the literature about the post-soil interaction based on experimental or numerical analyses. This is why the crash-test standards do not contain any details or details of the soil properties. The behavior of sigma-type posts under semi-static and dynamic loading on gravel soil were investigated with experimental and numerical modeling by Wu and Thomson [6]. They used a standard PED in the tests and modelled in the numerical analyses. Atahan and Cansız [2] analyzed the crash tests of the guardrails of circular wooden posts used in the United States. Full-scale crash-test results were simulated and detailed LS-DYNA analyses were carried out. It is recommended that the PED can be reduced in order to improve the behavior of the guardrail system and energy absorption. The behavior of a vehicle impacted guardrails applied on surfaces with variable inclination was investigated by Atahan [7]. The study was based on the crash effect of the vehicle existing in the slopes. In the study, the slopes are modelled as 1:1, 2:1, 4:1, 6:1, 8:1 and 10:1 (horizontal: vertical) and the stability of the vehicle and the adequacy of the guardrail system during the vehicle crash are examined using a software LS-DYNA program. The results showed that vehicles on 4:1 and more slopes could interact more securely with the guardrail system. A similar study was carried out by Marzougui et al. [8]. The purpose of this study is to investigate the use of rope guardrails in safety zones. The rope guardrails with different geometries, vehicles and surface inclinations

were studied as variables using the LS-DYNA program. Vehicle safety was studied and used to determine the most suitable configurations for rope guardrails. Polivka et al. [9] investigated the vehicle stability by driving a 2:1 (horizontal: vertical) slope guardrail system. The study involved an actual crash test and the guardrail system was able to stop the crashing vehicle safely. A study was conducted by Reid [5] to demonstrate road safety using the LS-DYNA program. In this study it was shown that how efficient the LS-DYNA program is and how accurately it can predict the dynamic interactions. Sheikh and Bligh [10] conducted a study on the effect of the inclination of the refugees on vehicle behavior and accordingly the selection of the concrete barrier locations. An optimization study was carried out on the selection of the location of concrete barriers for different slopes using the LS-DYNA program. In addition, Bonin et al. [11] and Atahan et al. [3] conducted a structural efficiency analysis of many road-safety structures using the LS-DYNA program. The structures examined in these studies are crossing guardrails, bridge barriers, energy-absorbing crash posts and guardrails. The effects of water content, lime content and compaction energy on the compaction characteristics of lime-treated loess highway embankments were investigated using laboratory and in-situ compaction tests [14]. The maximum dry density and the optimum water content of loess with different lime contents were determined. The results indicate that the maximum dry density increases due to the increase of the water content. It was also reported that a higher water content and compaction energy is needed for the optimum compaction. Woo et al. [15] used the conventional 3D finite-element approach and the hybrid approach that combines Lagrange and SPH (smoothed particle hydrodynamics) elements to evaluate the response of a laterally loaded single guardrail post with a square tube embedded in the sloping ground. They reported that these approaches seem to be suitable to model the ground slope, as well as to obtain the response of the soil-post system dominated by bending deformations. El-Maaty [16] investigated the effect of including different reinforcement types on reducing the rapid accumulation of pavement damage caused by freeze-thaw cycles or the low strength of a silty pavement foundation. The CBR strength and freeze-thaw behavior were tested with the inclusion of randomly distributed fibers, chemical additives and waste or by-product materials. It is concluded that the unsubmerged samples reinforced with waste materials provided a significant improvement in the CBR strength and the best performance was observed with the submerged samples treated with chemical additives of 10%. Grouting is an effective way to improve the strength characteristics significantly and can also contribute to the stabilization of sand. Gamil et al. [17] developed a

simulation and instrumental setup to be used for cement grouting. The shear strength of the sand was recorded before and after the grouting procedure. They reported that the shear strength increased after injecting the sand with cement and the setup produced accurate grouted samples with an even distribution of the cement mix. Hussain [18] examined the effect of the compaction energy of the engineering properties, i.e., compaction characteristics, unconfined compressive strength, California bearing ratio and the swell percentage of the soil. Substantial improvements in these properties were obtained in the tests. It is reported that compacting the soil at higher compaction energy levels can provide an effective approach to the stabilization of expansive soils up to a particular limit. The swell potential is increased due to the reduction in the permeability of the soil when the soil is compacted more than this limit.

As seen from studies in the literature, the design of the guardrail systems are planned without soil conditions. In general, a constant depth of guardrail is used regardless of the type of soil. Actually, the soil conditions directly affect the post embedment depths (PEDs) in steel guardrail systems. In other words, it is not a proper engineering approach to use the same PEDs for different soil characteristics. This study focused directly on the performance of the guardrails under different soil conditions. In this study, a series of field pendulum-impact tests were conducted in Iskenderun, Hatay, Turkey. These tests were performed on soil embedded posts to determine the optimum PED for three different soil conditions, i.e., hard, medium-hard and soft soil. A pendulum device was used to perform the dynamic impact tests on C-type (C120×60×4), H-type (C150×90×6) and S-type (S100×50×4.2) posts. Seven different PED values were used for each type of soil. These values are varied from 600 mm to 900 mm for C-type posts; varied from 700 mm to 1300 mm for H-type and S-type posts. A total of 63 impact tests performed proved that the increased soil stiffness resulted a reduction in the PED for the posts. Optimum PED values were determined based on the energy absorption of the posts. With the use of optimum-length guardrail posts a considerable amount of installation time, labor and material savings are expected.

## 2 FIELD TESTS

---

### 2.1 Site Characterization

Three different soil pits were prepared for the field impact testing. The dimensions of these pits were 1.0 m wide × 60.0 m long × 1.5 m deep, as shown in Figure 1. A total of 63 posts with 1.0 m spacing were installed



Figure 1. Preparation of soft, medium hard and hard soil pits for post installation.

in these three soil pits. The dimensions of the soil pits were selected based on the largest PED used in the study, potential post removal during tests, prevention of any interaction between posts and economic considerations.

The soil used in the pits represents the standard base granular material used by the Turkish Road Authorities [12]. To determine the geotechnical properties of the granular material to be used in these pits a series of laboratory tests, such as grain-size analysis, moisture content, field density, unit weight, shear box, standard and modified proctor tests were performed. The results of these experiments are presented in Table 1. The grading curve of the granular material used in the tests is given in Figure 2. After the laboratory tests, selected granular materials were used to construct the pits. Sand Cone and California Bearing Ratio tests were used to verify the density of the granular material for hard, medium-hard and soft soil conditions. The results of these field tests are listed in Table 2. As shown, acceptable soil stiffness levels were reached before the initiation of the post-installation procedure. At the same time, the density indices of the soil pits are 80%, 88% and 95% for the loose, medium-hard and hard soil conditions, respectively.

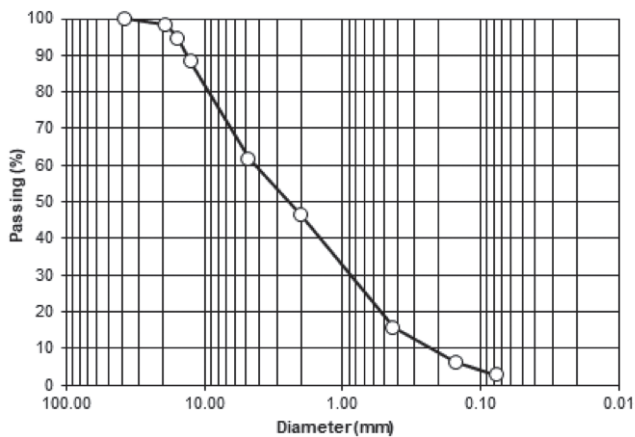


Figure 2. Grading curve of the granular material used in the tests.

Table 1. Geotechnical properties of the soil from laboratory tests.

Parameter	Property
Soil classification	SP (USCS); A3 (AASHTO); Sand (triangular classification)
Water content	4 %
Dry density	max: 21.0 kN/m <sup>3</sup> ; min: 16.0 kN/m <sup>3</sup>
Particle density	25.3 kN/m <sup>3</sup>
Internal friction angle	soft: 36°; medium hard: 44°; hard: 48°
Max. dry density and optimum water content (standard proctor test)	$\gamma_{kmax} = 21.0 \text{ kN/m}^3$ ; $\omega_{opt} = 8\%$
Max. dry density and optimum water content (modified proctor test)	$\gamma_{kmax} = 22.0 \text{ kN/m}^3$ ; $\omega_{opt} = 7\%$

Table 2. Geotechnical properties of the soil from field tests.

Name	Test Result
Sand Cone Test	Loose: 17.0 kN/m <sup>3</sup>
	Medium dense: 18.5 kN/m <sup>3</sup>
	Dense: 20.0 kN/m <sup>3</sup>
CBR Test	Loose: 36%
	Medium dense: 64%
	Dense: 95%

## 2.2 Details of guardrail posts used and experimental setup

Three different shaped posts, i.e., C-type (C120×60×4), H-type (H150×90×6) and S-type (S100×50×4.2) are used in this study. Typical views of the posts are given in Figure 3. As shown in Tables 3–5, the PED ranged from 650 mm to 900 mm for C-type posts, ranged from 700 mm to 1300 mm for H-type and S-type posts for all three soil conditions. In this table from the test codes, the letter gives the soil type and the numbers indicate the PED values. The posts were driven into the soil using a post-installation machine and a picture of the installation procedure is shown in Figure 4. To deliver the impact forces to the posts, a 1 kg pendulum device was

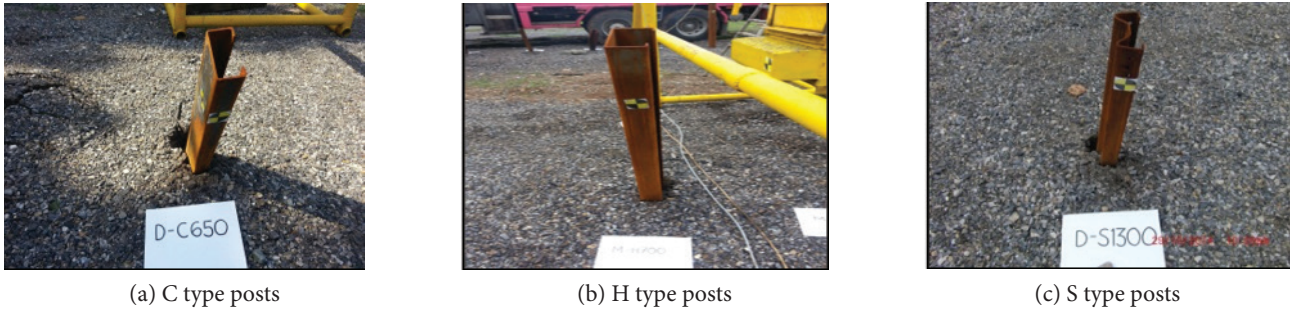


Figure 3. Typical views of the posts used in the study.

used. The pendulum was raised 1.5 m using an electric motor and the impacted posts about 550 mm above ground level. This distance represents the bumper height of an average small car. In this test setup, the pendulum applied 14.7 kJ of kinetic energy to the posts. A picture of the pendulum used in this study is shown in Figure 5. An accelerometer was installed on the pendulum to measure the acceleration-time history during impact. As shown in Figure 6, a data-acquisition system is setup to transfer the acceleration data in the *x*, *y* and *z* directions from

the accelerometer to an 8-channel data collector and from there to a computer. The acceleration-time histories for all 63 impact tests are recorded in Excel format. This history is used to calculate the velocity-time and eventually the displacement-time histories. The force is calculated based on the mass multiplied by the measured acceleration. Eventually, a force-displacement history is obtained from all 63 impact cases. The area under these curves represented the work done, in other words, the energy absorbed by the post-soil interaction.

Table 3. Details of guardrail posts tested (C type).

Post Designation	PED (mm)	Soil Characterization	Code	
C120x60x4	600	H (Hard)	H-600	
	650		H-650	
	700		H-700	
	750		H-750	
	800		H-800	
	850		H-850	
	900		H-900	
	600		M (Medium Hard)	M-600
	650			M-650
	700	M-700		
	750	M-750		
	800	M-800		
	850	M-850		
	900	M-900		
	600	S (Soft)		S-600
	650			S-650
	700		S-700	
	750		S-750	
800	S-800			
850	S-850			
900	S-900			

Table 4. Details of guardrail posts tested (H type).

Post Designation	PED (mm)	Soil Characterization	Code	
H150x90x6	700	H (Hard)	H-700	
	800		H-800	
	900		H-900	
	1000		H-1000	
	1100		H-1100	
	1200		H-1200	
	1300		H-1300	
	700		M (Medium Hard)	M-700
	800			M-800
	900	M-900		
	1000	M-1000		
	1100	M-1100		
	1200	M-1200		
	1300	M-1300		
	700	S (Soft)		S-600
	800			S-650
	900		S-700	
	1000		S-750	
1100	S-800			
1200	S-850			
1300	S-900			

**Table 5.** Details of guardrail posts tested (S type).

Post Designation	PED (mm)	Soil Characterization	Code
S100x50x4.2	700	H (Hard)	H-700
	800		H-800
	900		H-900
	1000		H-1000
	1100		H-1100
	1200		H-1200
	1300	H-1300	
	700	M (Medium Hard)	M-700
	800		M-800
	900		M-900
	1000		M-1000
	1100		M-1100
	1200		M-1200
1300	M-1300		
700	S (Soft)	S-600	
800		S-650	
900		S-700	
1000		S-750	
1100		S-800	
1200		S-850	
1300	S-900		



**Figure 4.** Installation of posts in soil.



**Figure 5.** Pendulum test device used in dynamic impact tests with three dimensional accelerometer.



**Figure 6.** Data acquisition setup used during dynamic pendulum testing (1) data cable between accelerometer and data collector box, (2) 8-channel data collector, (3) recording data in a computer.

### 3 TEST RESULTS AND DISCUSSION

#### 3.1 Visual inspections

A total of 63 impact tests were performed using the pendulum device. Each of the test results was recorded visually and analytically. The general views for the different soil conditions (soft-S, medium hard-M and hard-H soil) after the tests where C-type posts were used are given in Figure 7. And then a qualitative evaluation of all the tests is presented in Tables 6-8. In general, when an insufficient PED is used the posts exhibited an upwards movement and in some cases were almost completely removed from the soil. On the other hand, when sufficient PED is used, the posts remained in the soil with minimal upward motion and in some cases post buckling was observed.

**Table 6.** Qualitative evaluation of the pendulum test results (C-type post).

PED (mm)	Soil Stiffness		
	Hard (H)	Medium hard (M)	Soft (S)
600	1 The post moved upwards in the ground, but was not completely removed from the soil. The soil body is collapsed. The pendulum slowed down after impact	Same as H-600	The post moved upwards in the ground and completely removed from the soil. The soil body is collapsed. The pendulum movement continued.
650	The post movement in the soil is less than H-600, but the soil body is collapsed. The pendulum stopped after the impact.	Same as M-600	Same as S-600
700	The post's upwards movement is not observed and minimal soil movement occurred. The post-soil interaction and energy absorption are acceptable.	Somewhat improvement compared to the M-650 case. The soil body is collapsed. The pendulum stopped after the impact.	Same as H-600
750	Due to sufficient PED, slight post buckling is observed. Post-soil interaction and energy absorption are acceptable.	Same as H-700	Same as M-700
800	Post buckling becomes more visible. Post-soil interaction and energy absorption is acceptable.	Same as H-750	Same as H-700
850	Same as H-800	Same as H-800	Same as H-800
900	Same as H-800	Same as H-800	Same as H-800

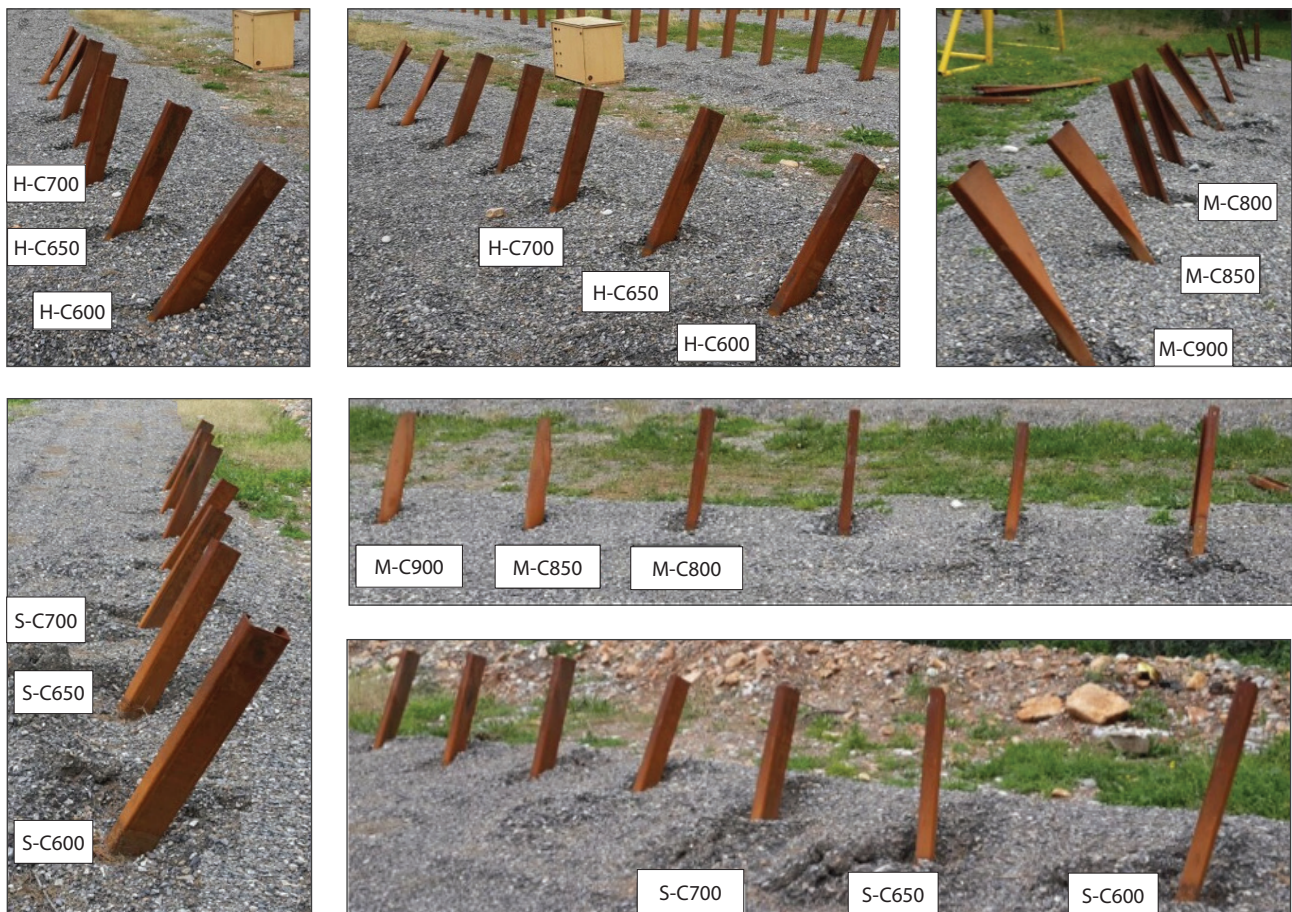


**Figure 7.** General views of the soil for C-type posts after the impact tests.

**Table 7.** Qualitative evaluation of the pendulum test results (H-type post).

PED (mm)	Soil Stiffness		
	Hard (H)	Medium hard (M)	Soft (S)
700	The post moved upwards in the ground but was not completely removed from the soil. The soil body is collapsed. The pendulum movement continued.	The post moved upwards in the ground and the soil body collapsed. The pendulum movement continued.	The maximum post movement was observed and the soil body collapsed. The pendulum movement continued.
800	The post movement in the soil is less than H-700, but the soil body is collapsed. The pendulum stopped after the impact.	The post movement in the soil is less than M-700 and the soil body is collapsed. The pendulum stopped after the impact.	The post movement in the soil is less than S-700 and the soil body is collapsed.
900	Due to sufficient PED, slight post buckling is observed. Post-soil interaction and energy absorption are acceptable.	Due to sufficient PED, slight post buckling is observed. Post-soil interaction and energy absorption are acceptable.	Due to sufficient PED, slight post buckling is observed. The post movement in soil is great compared with hard and medium-hard soil types.
1000	Post-soil interaction and energy absorption are acceptable.	Same as H-1000	Same as H-1000
1100	Same as H-1000	Same as H-1000	Same as H-1000
1200	Same as H-1000	Same as H-1000	Same as H-1000
1300	Same as H-1000	Same as H-1000	Same as H-1000

**Table 8.** Qualitative evaluation of the pendulum test results (S-type post).

PED (mm)	Soil Stiffness		
	Hard (H)	Medium hard (M)	Soft (S)
700	The post moved upwards in the ground, but was not completely removed from the soil. The soil body is collapsed. The pendulum movement continued.	Same as H-700	The maximum post movement was observed and the soil body collapsed. The pendulum movement continued.
800	The post movement in the soil is less than H-700, but the soil body collapsed. The pendulum stopped after impact.	Same as H-800	The post movement in the soil is less than S-700 and the soil body collapsed. The pendulum movement continued.
900	The post's upwards movement is not observed and minimal soil movement occurred. Post-soil interaction and energy absorption are acceptable.	Same as H-900	The post movement in the soil is less than S-800, but the soil body is collapsed. The pendulum stopped after the impact.
1000	Due to sufficient PED, slight post buckling is observed. Post-soil interaction and energy absorption are acceptable.	Same as H-1000	Same as H-1000
1100	Post buckling becomes more visible. Soil movement is negligible.	The post's upwards movement is not observed and minimal soil movement occurred.	Same as H-1100
1200	Post buckling becomes more visible.	Due to sufficient PED, slight post buckling is observed.	Same as M-1100
1300	Same as H-1200	Same as H-1200	Same as M-1200

### 3.2 Analytical Calculations

The maximum measured accelerations and the energy absorbed, calculated using the area under the force-deformation curve for all 63 impact tests, are presented in Table 9. In the pendulum test, the mass of 750kg

was lifted 1.5m each time and then released free. A kinetic energy of 11.04 kJ was applied to the posts by the pendulum. This value was determined using the standard kinetic energy formula after calculating the velocity that the post had just before the impact. Compared to the energy levels applied to the guardrail systems by the vehi-



**Table 9.** Maximum energy absorption and acceleration calculations for the pendulum tests.

Post type	PED (mm)	Soil Stiffness					
		Hard (H)		Medium hard (M)		Soft (S)	
		Max. Energy Absorbed (kJ)	Max. Accel. (g)	Max. Energy Absorbed (kJ)	Max. Accel. (g)	Max. Energy Absorbed (kJ)	Max. Accel. (g)
C120×60×4 (C)	600	0.72	- 2.88	0.66	- 2.06	0.49	- 1.08
	650	2.93	- 4.05	2.11	- 2.90	1.77	- 2.45
	700	3.27	- 4.52	2.35	- 3.25	2.14	- 2.96
	750	4.58	- 6.33	3.29	- 4.55	2.89	- 3.99
	800	5.75	- 11.95	4.14	-10.72	3.31	- 7.93
	850	6.86	- 18.48	4.94	-16.83	4.01	- 13.54
	900	7.92	- 25.85	6.13	-24.47	5.19	- 18.87
C150×90×6 (H)	700	10.03	-34.81	9.56	-33.21	8.89	-31.65
	800	10.65	-35.05	10.12	-34.54	9.34	-32.68
	900	11.04	-35.26	10.74	-35.12	10.01	-33.84
	1000	11.04	-35.32	11.04	-35.51	10.71	-34.82
	1100	11.04	-35.45	11.04	-35.47	11.04	-35.21
	1200	11.04	-35.41	11.04	-35.61	11.04	-35.52
	1300	11.04	-35.56	11.04	-35.55	11.04	-35.49
C100×50×4.2 (S)	700	3.32	-4.59	3.07	-4.24	0.92	-1.27
	800	5.31	-7.34	5.11	-7.06	2.22	-3.07
	900	6.61	-9.14	6.39	-8.83	2.95	-4.08
	1000	7.51	-10.38	7.17	-9.91	3.61	-8.99
	1100	8.05	-18.13	7.77	-17.74	4.26	-15.89
	1200	8.44	-19.67	8.01	-18.07	6.03	-16.84
	1300	9.61	-25.28	8.31	-23.21	7.93	-21.75

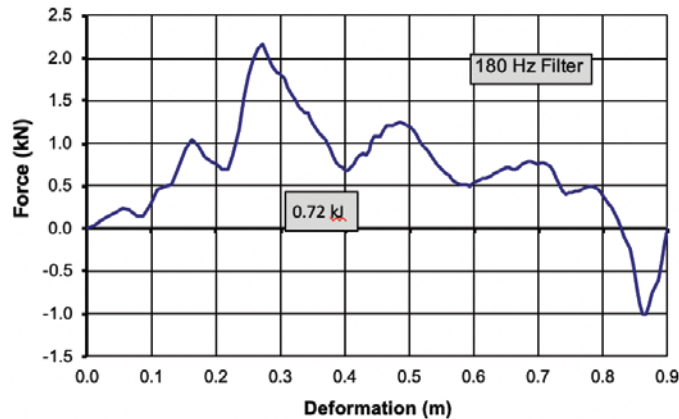


**Figure 8.** Typical force-deformation curve after the impact test.

cles in the actual crash tests, the 11.04 kJ is a reasonable energy level that can be used to determine the impact behavior of the post driven into the soil. The following equations were used to calculate the energy level.

$$m g h = 0.5 m V^2 \quad (1)$$

$$V = (2 g h)^{0.5} = (2 \times 9.81 \times 1.5)^{0.5} = 5.43 \text{ m/s} \quad (2)$$

$$E = 0.5 m V^2 = 0.5 \times 750 \times 5.43^2 = 11.04 \text{ kJoule} \quad (3)$$

During the impact, this energy is absorbed by the post and the absorption depends directly on the post material's strength, the PED and the soil properties. The impact of the pendulum on the posts means that all its energy transmits to the post. A typical force-deformation curve is given in Figure 8 for the C-type posts, 600mm of PED and the hard-soil condition.

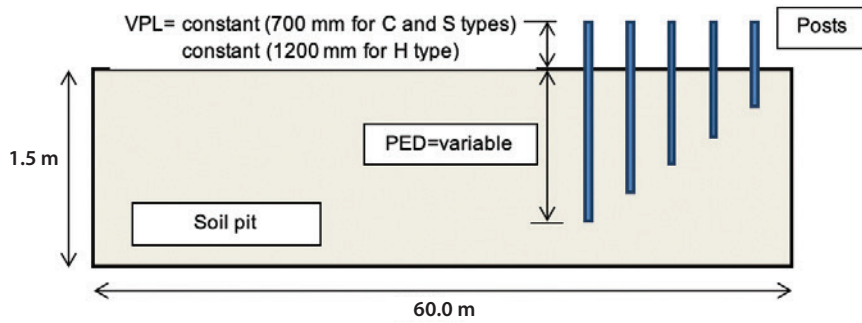


Figure 9. Cross-sections of the soil pits and the PEDs.

#### 4 EVALUATION OF FIELD TEST RESULTS

In this study, three different post shapes, i.e., C type (C120×60×4), H type (H150×90×6) and S type (S100×50×4.2) are used. The PED ranged from 650 mm to 900 mm for the C-type posts and ranged from 700 mm to 1300 mm for the H-type and S-type posts for all three soil conditions. The visible post length (VPL) above the soil was kept constant at 700 mm for the C- and S-type posts and 1200 mm for the H-type post. Figure 9 shows cross-sections of the soil pits and PEDs.

The posts were embedded in soft, medium-hard and hard soil conditions, for which the soil properties are given above. The relations of the post embedment depth/visible post length (PED/VPL), energy-absorption capacity (EAC) for different soil (soft, medium-hard and hard) and post types (C, H and S type) are given in Figure 10. As shown in this figure, there is a linear relationship between the PED/VPL ratio and the magnitude of the energy-absorption capacity increases when the PED/VPL ratio increases for all the types of soil and post. For the C-type posts given in Figure 10a, the energy-absorption capacity increases from 4.44% to 47.01% when the PED increases from 600 mm to 900 mm in a soft-soil environment. Similarly, in the case of medium-hard soil, when the PED increases from 600 mm to 900 mm, the energy-absorption capacity increases from 5.98% to 55.53%. In the hard-soil conditions, this value increases from 6.52% to 71.74%. Similar observations are obtained for the H-type and S-type posts, given in Figure 10b and c.

The internal friction angle of the soil ( $\phi$ ) – EAC (%) relation of the C-, H- and S-type posts that embedded in soft, medium-hard and hard soils are presented in Figure 11. These relationships are given for different PED values. In these figures, the soft, medium-hard and hard soils are represented by internal friction angles of 36°, 44° and 48°, respectively. As shown in these figures there is a linear relationship between the internal fric-

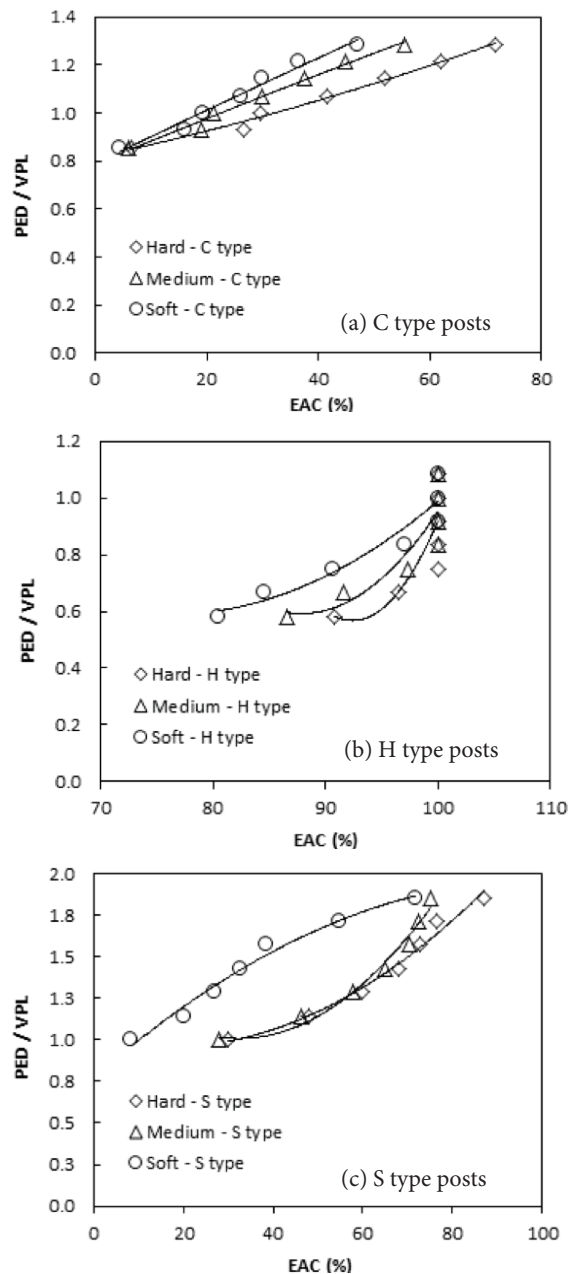


Figure 10. EAC-PED/VPL relationship according to the soil conditions.

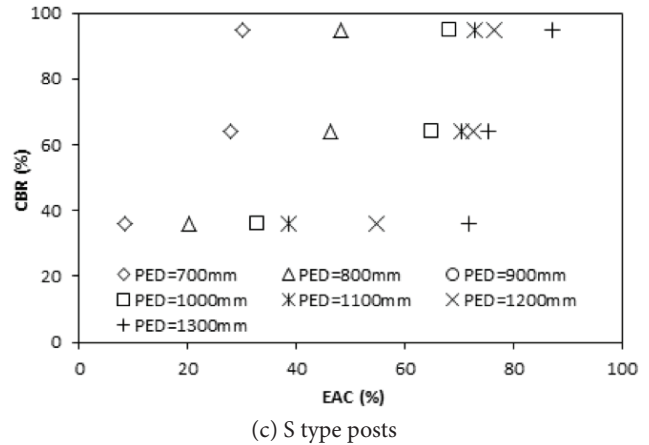
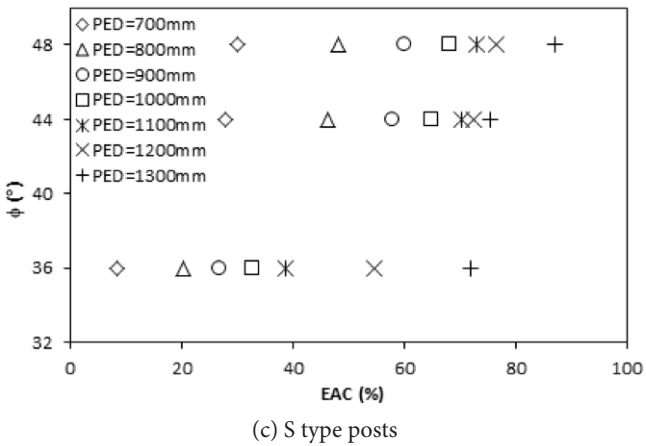
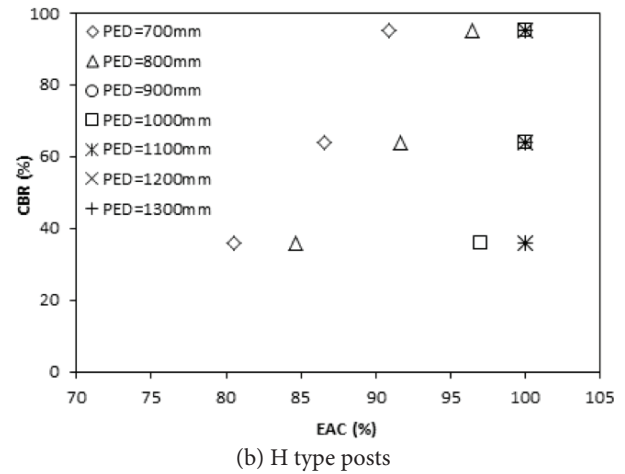
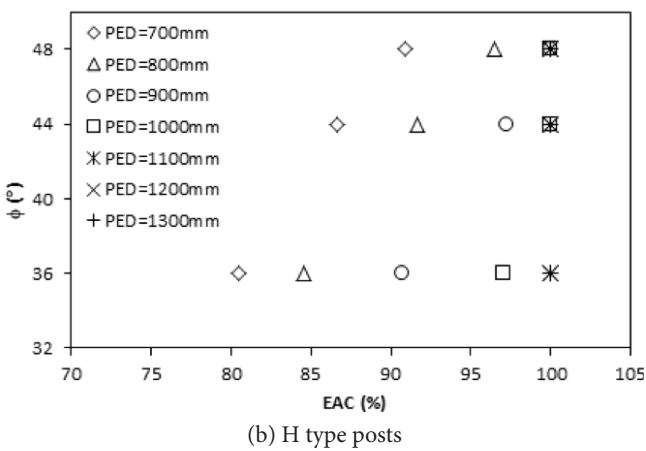
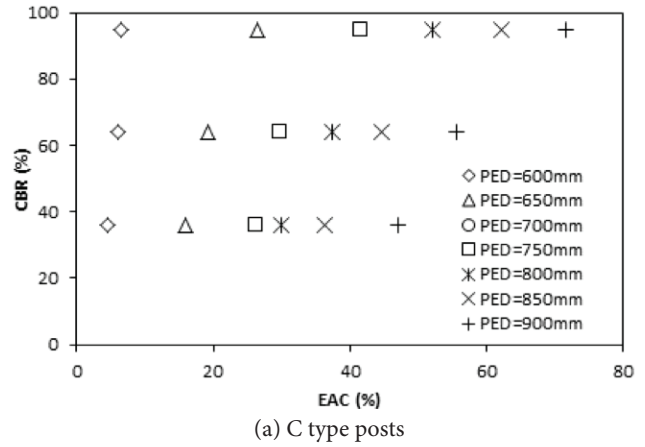
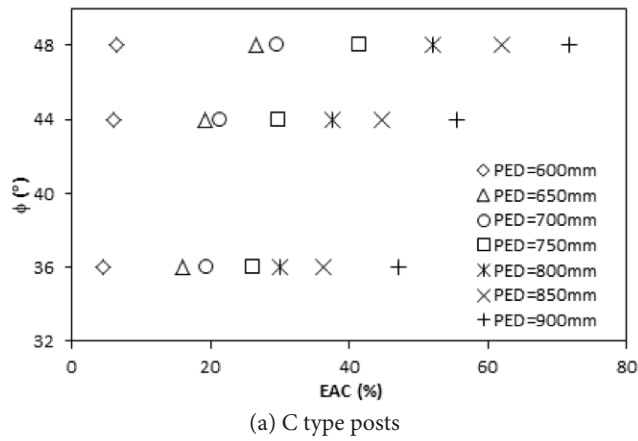


Figure 11. EAC- $\phi$  relationship according to the PED values.

Figure 12. EAC-CBR relationship according to the PED values.

tion angle and the magnitude of the energy-absorption capacity. Note that the EAC increases when  $\phi$  increases for all the types of soil and post. For the H-type posts given in Figure 11b, the energy-absorption capacities are 97.01%, 100.0% and 100.0%, for the soft ( $\phi=36^\circ$ ), medium-hard ( $\phi=44^\circ$ ) and hard ( $\phi=48^\circ$ ) soil conditions,

respectively. For the same soil stiffness (for example,  $\phi=48^\circ$ ) the energy-absorption capacity increases with an increase in a certain value of the PED and then it remains constant. For the H-type posts, for PED values 700 mm, 1000 mm and 1300 mm, the EAS are 90.85%, 100.0% and 100.0%, respectively.

The European crash-test standard EN1317 is a performance-based standard. In other words, the impact-response behavior of the guardrail designs are considered, regardless of the guardrail material, geometry or soil properties. This study focused on this phenomenon and evaluated the safety performance of the guardrail posts when they are installed into various soil types, such as soft, medium-hard and hard. In this study it is agreed that the post behaves in a similar way to laterally loaded piles [13]. In the case of axially loaded piles, loads are transferred to the soil by shaft friction and base resistance. This total resistance resulted from the shaft resistance and end-bearing resistance, providing the equilibrium conditions. In the end-bearing piles, it is essential to have the pile base inserted into a stronger soil layer, such as dense sand, stiff clay or rock. If no such strong layer is available at the site, then the loads are carried only by the shaft friction. In the laterally loaded pile phenomenon, piles behave as transversely loaded beams. The lateral load is transferred to the surrounding soil mass by using the lateral resistance of the soil. A part or complete pile tends to shift horizontally in the direction of the applied load, causing pile bending, pile rotation or pile translation, depending on the post's stiffness, load value and soil property. The soil mass lying in the direction of the applied load generates compressive and shear stresses and strains in the soil that offers resistance to the pile movement. The soil-based results are interpreted in terms of the laterally loaded pile mechanism. In the current study, dynamic pendulum tests were performed to determine the optimum PED values for different soil conditions. Based on a total of 63 test results, the suggested optimum PED values for different types of soil and posts are given in Table 10, including the application standard. As seen clearly from Table 10, the optimum PEDs suggested in this study are smaller than the applied ones, especially in the hard and medium-hard soil conditions.

**Table 10.** Suggested and applied PED values.

Post	Optimum post embedment depth (PED <sub>opt</sub> )		
	Hard soil	Medium-Hard soil	Soft soil
PED <sub>suggested</sub> / PED <sub>applied</sub>			
C type	750mm / 950mm	850mm / 950mm	950mm / 950mm
S type	1000mm / 1200mm	1100mm / 1200mm	1200mm / 1200mm
H type	800mm / 1230mm	900mm / 1230mm	1000mm / 1230mm

Table 11 gives the amount of saving percentages for one post for each type of post and soil used. It was determined that significant savings were made, especially in C- and H-type posts and also for hard-soil conditions. Considering the optimum length in the guardrail post

design, significant savings can be achieved for a mile of road. In other words, with the use of the optimum length of guardrail posts, a considerable amount of installation time, labor and material savings are expected. This study has shown that the optimum embedment depths of the guardrail posts can be decided by determining the soil properties in the light of the standard geotechnical experiments to be performed on the roads where the guardrail post is to be installed.

**Table 11.** Amount of savings according to PED<sub>opt</sub>.

Post	Hard soil	Medium-Hard soil	Soft soil
C type	21.05%	10.53%	0.00%
S type	16.67%	8.33%	0.00%
H type	34.96%	26.83%	18.70%

## 5 CONCLUSIONS

In this study a series of field pendulum-impact tests were performed on soil-embedded posts to determine the optimum PED for three different soil conditions, namely, hard, medium-hard and soft soil. A pendulum device was used to perform the dynamic impact tests on C-type (C120×60×4), H-type (C150×90×6) and S-type (S100×50×4.2) posts with seven different PED values used for each type of soil. Based on the research findings, the following specific conclusions can be drawn:

- Dynamic pendulum tests proved that an increased soil stiffness resulted in a reduction in PED for the posts due to an improved post-soil interaction.
- It is determined that the posts tend to move upwards, get out of the soil quickly and thus could not provide enough resistance when the PED is insufficient.
- Soil stiffness has an important effect on the impact-response behavior of the guardrail posts. There is a linear relationship between the internal friction angle and the magnitude of the energy-absorption capacity increases when  $\phi$  increases for all the types of soil and post. Similar behavior was observed from a CBR perspective.
- It has been determined that significant savings have been made, especially in C- and H-type posts and also for hard soil conditions.
- When comparing the optimum values with the standards, the savings obtained for hard soils can reach up to 35% for H-type posts. These savings are about 20% for C-type posts and about 15% for S-type posts.
- Considering the larger PED in similar guardrail systems in use today, designs with optimum PED will help save a considerable amount of installation time, labor and material.

## Acknowledgments

The work presented in this paper was carried out with funding from TUBITAK (Scientific and Technological Research Council of Turkey), Grant No. 213M516.

## REFERENCES

- [1] AASHTO. 2014. Roadside design guide. American Association for State Highway and Transportation Officials. 4th Edition, Washington, D.C.
- [2] Atahan, A.O., Cansız, Ö.F. 2005. Improvements to G4(RW) strong-post round-wood W-beam guardrail system. *ASCE Journal of Transportation Engineering* 131(1), 63-73. DOI: 10.1061/(asce)0733-947x(2005)131:1(63)
- [3] Atahan, A.O., Bonin, G., Cicinnati, L., Yaşarer, H.I. 2008. Development of a crashworthy end terminal TWINY for three-beam guardrail. *ASCE Journal of Transportation Engineering* 133(4), 467-476. DOI: 10.1061/(ASCE)0733-947X(2008)134:11(467)
- [4] CEN. 2017. European Crash Testing Standard EN1317. Performance classes, impact test acceptance criteria and test methods for safety barriers, Brussels.
- [5] Reid, J.D. 2004. LS-DYNA simulation influence on roadside hardware. Transportation Research Board Annual Meeting, Paper No. 04-2619, Washington D.C. DOI: 10.3141/1890-04
- [6] Wu, W., Thomson, R.A. 2007. A study of the interaction between a guardrail post and soil during quasi-static and dynamic loading. *International Journal of Impact Engineering* 34, 883-98. DOI: 10.1016/j.ijimpeng.2006.04.004
- [7] Atahan, A.O. 2003. Impact behavior of G2 steel weak-post W-beam guardrail on nonlevel terrain. *Heavy Vehicle Systems, A series of the International Journal of Vehicle Design* 10(3), 209-223. DOI: 10.1504/IJHVS.2003.003207
- [8] Marzougui, D., Mohan, P., Kan, C.D., Opiela, K.S. 2007. Performance evaluation of low tension three strand cable median barriers, Transportation Research Board Annual Meeting, Washington D.C. DOI: 10.3141/2025-03
- [9] Polivka, K.A., Sicking, D.L., Faller, R.K., Bielenberg, R.W. 2000. Development of a W-beam guardrail system for use on a 2:1 Slope. *Transportation Research Record* 1743, 80-87.
- [10] Sheikh, N.M., Bligh, R.P. 2006. Analysis of the impact performance of concrete median barrier placed on or adjacent to slopes, Report No. FHWA/TX-06/0-5210-1, Texas A&M University, Texas.
- [11] Bonin, G., Cantiasani, G., Loprencipe, G., Ranzo, A., Atahan, A.O. 2009. Retrofit of an existing Italian bridge rail for H4a containment level using simulation, *Heavy Vehicle Systems, A series of the International Journal of Vehicle Design* 16(1/2), 258-270. DOI: 10.1504/IJHVS.2009.023864
- [12] TRA. 2016. Handbook of properties of road construction materials. General Directorate of Turkish Roads, Turkish Road Association, Ankara, Turkey.
- [13] Teng, T.L., Liang, C.C., Hsu, C.Y., Shih, C.J., Tran, T.T. 2016. Effect of soil properties on safety performance of Wbeam guardrail. *International Conference on Advanced Material Science and Environmental Engineering (AMSEE 2016)*, 34-36. DOI: 10.2991/amsee-16.2016.10
- [14] Zhang, Y., Ye, W., Wang, Z. 2017. Study on the compaction effect factors of lime-treated loess highway embankments. *Civil Engineering Journal* 3(11), 1008-1019. DOI: 10.28991/cej-030933
- [15] Woo, K.W., Lee, D.W., Ahn, J.S. 2018. Impact behavior of a laterally loaded guardrail post near slopes by hybrid SPH model. *Advances in Civil Engineering*, Article ID 9479452, 12 pp. DOI: 10.1155/2018/9479452
- [16] El-Maaty, A.E. 2016. Enhancing the CBR strength and freeze-thaw performance of silty subgrade using three reinforcement categories. *Civil Engineering Journal* 2(3), 73-85.
- [17] Gamil, Y., Bakar, I., Ahmed, K. 2017. Simulation and development of instrumental setup to be used for cement grouting of sand soil. *Italian Journal of Science and Engineering* 1(1), 16-27.
- [18] Hussain, S. 2017. Effect of compaction energy on engineering properties of expansive soil. *Civil Engineering Journal* 3(8), 610-646. DOI: 10.28991/cej-030988